Space Sci Rev
DOI 10.1007/s11214-015-0195-2

The Solar Extreme Ultraviolet Monitor for MAVEN

F.G. Eparvier[1] · P.C. Chamberlin[2] · T.N. Woods[1] · E.M.B. Thiemann[1]

Received: 17 November 2014 / Accepted: 30 July 2015

Abstract The Extreme Ultraviolet (EUV) monitor is an instrument on the NASA Mars Atmosphere and Volatile EvolutioN (MAVEN) mission, designed to measure the variability of the solar soft x-rays and EUV irradiance at Mars. The solar output in this wavelength range is a primary energy input to the Mars atmosphere and a driver for the processes leading to atmospheric escape. The MAVEN EUV monitor consists of three broadband radiometers. The radiometers consist of silicon photodiodes with different bandpass-limiting filters for each channel. The filters for the radiometers are: Channel A: thin foil C/Al/Nb/C for 0.1–3 nm and 17–22 nm, Channel B: thin foil C/Al/Ti/C for 0.1–7 nm, and Channel C: interference filter for 121–122 nm. A fourth, covered photodiode is used to monitor variations in dark signal due to temperature and radiation background changes. The three science channels will monitor emissions from the highly variable corona and transition region of the solar atmosphere. The EUV monitor is mounted on the top deck of the MAVEN spacecraft and is pointed at the Sun for most of its orbit around Mars. The measurement cadence is 1-second. The broadband irradiances can be used to monitor the most rapid changes in solar irradiance due to flares. In combination with time-interpolated observations at Earth of slower varying solar spectral emissions, the broadband MAVEN EUV monitor measurements will also be used in a spectral irradiance model to generate the full EUV spectrum at Mars from 0 to 190 nm in 1-nm bins on a time cadence of 1-minute and daily averages.

Keywords Solar irradiance · Extreme ultraviolet · Mars · MAVEN

✉ F.G. Eparvier
eparvier@colorado.edu

P.C. Chamberlin
phillip.c.chamberlin@nasa.gov

T.N. Woods
tom.woods@lasp.colorado.edu

E.M.B. Thiemann
ed.thiemann@lasp.colorado.edu

[1] Laboratory for Atmospheric & Space Physics, University of Colorado, Boulder, CO, USA

[2] NASA Goddard Spaceflight Center, Greenbelt, MD, USA

Published online: 01 September 2015

1 Introduction

The Mars Atmosphere and Volatile EvolutioN (MAVEN) mission was launched in November 2013 and arrived at Mars in September 2014. A main goal of the MAVEN mission is to understand the escape of atmospheric species. The solar extreme ultraviolet (EUV) irradiance is one of the primary energy inputs to the Mars atmosphere. EUV light causes heating, ionization, and dissociation of the atoms and molecules in the upper atmosphere, all of which directly or indirectly contribute to atmospheric escape. The solar output in the EUV varies as a function of wavelength and on all timescales (such as solar cycle, solar rotation, and solar flares). This variability is a result of the magnetic activity on the Sun (Lean et al. 2011; Woods and Rottman 2002). Because this magnetic activity is unevenly distributed about the rotating Sun and is constantly evolving in time, solar irradiance at any point in the solar system depends on the distribution of activity on the face of the Sun toward that point, which may be different than the activity on the face of the Sun as seen from Earth orbit, where most solar EUV instrumentation is currently observing; hence the desire for a solar EUV monitor actually at Mars during the MAVEN mission.

2 EUV Instrument Overview

The EUV monitor for MAVEN is a part of Langmuir Probe and Waves (LPW) experiment (Andersson et al. 2014, this issue), which, in turn, is part of the Particles and Fields Package (PFP). The EUV monitor is a simple instrument consisting of filter radiometers to measure solar irradiance in three broad wavelength bands. The radiometers consist of photodiodes with bandpass-limiting filters to isolate wavelength ranges of interest in the solar irradiance. Similar instruments have flown on the Student Nitric Oxide Explorer (SNOE) mission (Bailey et al. 2000), the Thermosphere Ionosphere Mesosphere Energetics and Dynamics (TIMED) (Woods et al. 2005a), and the Solar Radiation and Climate Experiment (SORCE) (Woods et al. 2005b).

The detectors are silicon AXUV-100 photodiodes that are available commercially from Optodiode (formerly from International Radiation Detectors). The photodiodes are described in detail by Korde and Geist (1987), Korde et al. (1988), and Gullikson et al. (1996).

The filters vary by channel. Channels A and B have custom thin foil filters of multiple layers of materials made by Luxel mounted in front of the detectors. Channel A has C/Al/Nb/C layers of thicknesses: 25 nm of C, 250 nm of Al, 50 nm of Nb, and 25 nm C. The these thicknesses were chosen to match that of similar channels on the TIMED and SORCE instruments. Channel B has C/Al/Ti/C layers of thicknesses: 20 nm of C, 150 nm of Al, 300 nm of Ti, and 20 nm of C. The thicknesses for the Channel B filter were chosen to match a channel on the Solar Dynamics Observatory (SDO) EUV Variability Experiment (EVE) EUV Spectro-Photometer (ESP) instrument (Woods et al. 2012). Carbon is used as the outside layer for both sides of the foil filters to prevent oxidation of the metals. Channel C has a stack of two commercially available 122-XN interference filters made by Princeton Instruments (formerly Acton Optics). Two interference filters are used to reduce the visible solar light reaching the detector on this channel. In addition, the filters are tilted at 10° relative to the detector to limit re-entrant light.

A fourth silicon photodiode detector (Channel D) with no aperture or illumination path to the sun is included in the instrument to monitor changes in dark signals due to temperature and particle radiation. Also included in the EUV monitor is a bi-stable mechanism that, when in the "open" position, allows sunlight to be directly incident on the front apertures and filters

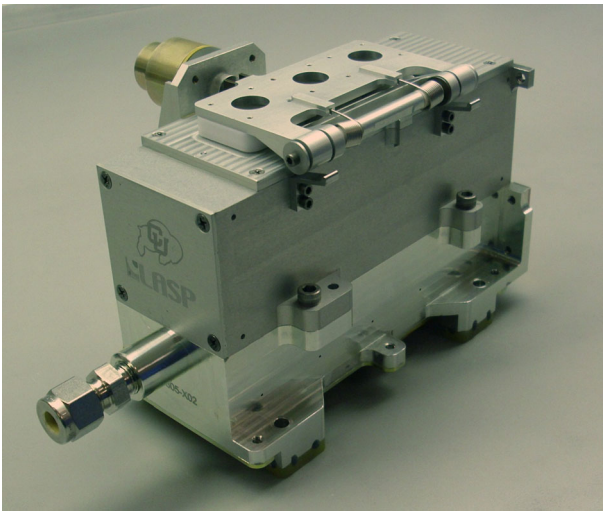

Fig. 1 The MAVEN EUV monitor shown on a lab-bench with the one-shot door closed

of the EUV monitor science channels. When in the "closed" position, the mechanism places fused silica windows in front of the science apertures. These windows allow visible light through, but block soft X-ray and EUV light. This allows for estimation of the out-of-band contribution to each channel's signal.

The bandpasses of the three science channels so that the signals in each channel were representative of differently varying emission regions in the solar atmosphere. Channel C isolates the bright H I Lyman-α emission at 121.6 nm that has its origin in the transition region and varies from a few percent during flares to 10–100 % over times scales of months and years (Woods et al. 2000). It can be used as a proxy for other transition region emissions in the solar spectrum, similar to, but improved upon the common F10.7 index. Channel B is sensitive in the 0.1–7 nm range which is dominated by emissions from the hot solar corona and that can vary by several orders of magnitude on the timescales of solar flares. This channel can be used as a proxy for other flaring emissions similar to the GOES 0.1–0.8 nm soft X-ray index. Finally, Channel A is sensitive in the 0.1–3 nm and 17–22 nm wavelength ranges. The short wavelength contribution can be approximated from the Channel B measurements, leaving the longer 17–22 nm wavelength signal that has origins in the cooler solar corona that can also vary by orders of magnitude during flares, but differently than the hot corona.

The EUV monitor radiometers, the preamplifiers, the bi-stable mechanism, and a one-shot door are packaged in a small housing that is shown in Fig. 1. The housing is 9.7 cm wide by 14.5 cm long by 10.9 cm tall. The one-shot door has fused silica windows that allowed for visible verification of mechanism motion during testing on the ground. Due to contamination concerns, the instrument was supplied with a dry nitrogen purge throughout ground testing and on the spacecraft up until launch. The mass of the EUV (without cabling) is 1.03 kg. The power consumption is 0.16 Watts (without heaters).

The location of the EUV monitor on the MAVEN spacecraft is shown in Fig. 2. Because of its location on the top deck of the spacecraft, whenever solar panels are pointed at the Sun, so too is the EUV monitor. The EUV channels have a conical science field of view of 2° (half-cone) and a glint-free field-of-view of 7.7° (half-cone).

Each photodiode detector in the EUV monitor has an Analog Devices AD549 pre-amplifier mounted in close proximity. The EUV monitor is connected to the Particles and

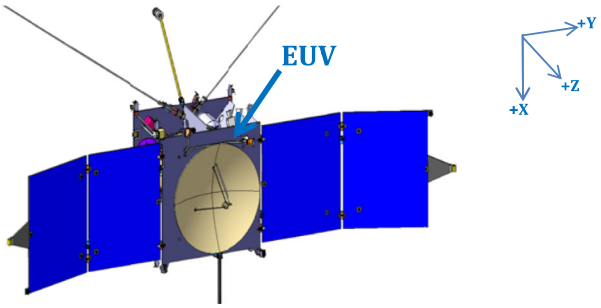

Fig. 2 The location of the MAVEN EUV monitor on the sun-facing deck of the spacecraft

Fields Digital Processing Unit (PFDPU) by a two meter harness. (See Fig. 1 of Andersson et al. (2014, this issue) for a block diagram of the LPW, EUV, and the associated electronics boards within the PFDPU.) The amplified EUV detector currents are read and processed in the PFDPU similar to the LPW sensor data as described by Andersson et al. (2014, this issue). The EUV sensor currents plus the current from a cryodiode temperature sensor mounted near the photodiodes are converted to voltages and sampled at 1 kHz by the Digital Fields Board (DFB) in the PFDPU. In the DFB the signals are filtered and averaged to 1-second cadence to dampen noise and reduce telemetry rate. The EUV photodiode and temperature measurements are then packetized along with the LPW data and transferred to the PFDPU for either on-board storage or transmission through telemetry. The PFDPU also controls the EUV aperture mechanism in response to commands passed on by the spacecraft. The one-shot EUV door and heaters mounted on the EUV sensor housing are controlled by the spacecraft.

3 Pre-flight Calibrations

The signal ($S_{tot,i}$ in Data Numbers (DN)) that gets sent down through telemetry from a channel i in the EUV monitor is given by:

$$S_{tot,i} = (I_{tot,i} \cdot G_{EUV,i} + V_{offset,i}) \cdot G_{DFB,i} + S_{offset},$$

where $I_{tot,i}$ is the total current in Amps from the detector in channel i, $G_{EUV,i}$ is the sensor gain in Volts/Amp, $V_{offset,i}$ is the offset in Volts applied to set the dark signal level, $G_{DFB,i}$ is the gain in the DFB in (DN/Volt), and S_{offset} is another offset ($= -4.4 \times 105$ DN) applied in the DFB to make the EUV signals more like the LPW signals in telemetry. The gains and offsets were measured as functions of temperature during ground testing and are to be confirmed in flight.

The total throughput of the EUV monitor science channels was calibrated at the National Institutes of Standards and Technology (NIST) Synchrotron Ultraviolet Radiation Facility-III (SURF-III) in Gaithersburg, MD in April and September 2013 (before and after environmental testing of the EUV instrument). SURF operates a 0.8 m radius electron storage ring with ten beamlines for observing the synchrotron radiation generated by the stored, orbiting electrons. Beamline 2 (BL-2) offers an unfiltered, unobstructed view of the beam. The EUV instrument was mounted inside a vacuum chamber at the end of the beamline, approximately 17.8 m from the light source. The entire BL-2 chamber can be translated horizontally (X) and vertically (Y) to illuminate different parts of the detector. Inside the chamber, the fully-integrated EUV monitor in a thermal controlled hut is mounted on

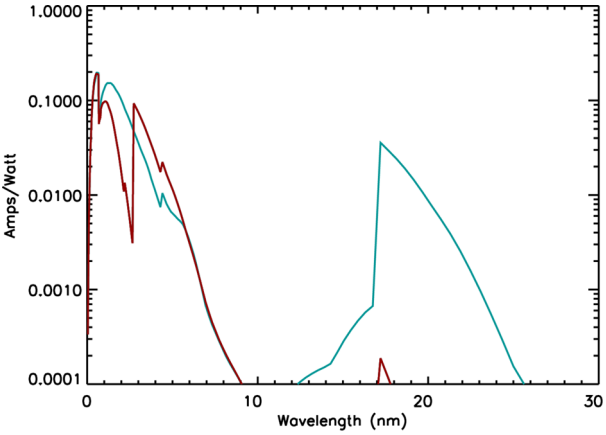

Fig. 3 The modeled wavelength responses for Channel A (*blue*) and Channel B (*red*)

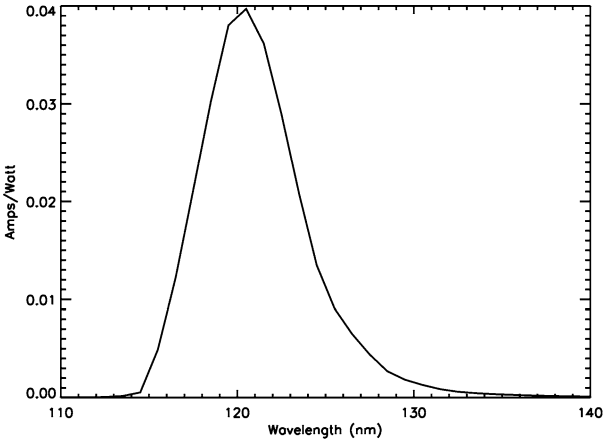

Fig. 4 The modeled wavelength response for Channel C

a Yaw/Pitch gimbal assembly which allows two-axis rotation at a given (X, Y) position, for mapping of the field of view (FOV). Trim magnets in the SURF ring control the average energy of the stored electrons moving around the ring. The resultant synchrotron beam spectrum depends on the electron energy with higher electron energies yielding spectra peaked at higher energies (shorter wavelengths).

The beam energies used for the EUV monitor calibrations were 285, 331, 380, and 408 MeV, having a spectral peak near 11, 7, 4.5, and 3.7 nm, respectively. Channels A and B were calibrated at each of the four beam energies. A model of the expected signal using the transmissions of the foil filters layers (Henke et al. 1993) and the response of the silicon photodiodes is run, iterating the filter layer thicknesses until a minimum difference is found for all results from the four beam energies. This iteration is done to determine the actual effective thicknesses of the layers in the foil filters instead of the requested thicknesses. The wavelength responses for the best fit to Channels A and B are shown in Fig. 3.

For Channel C only the 285 MeV beam energy was used because the bandpass is narrow enough to render the multiple energy method ineffective and the signal within the bandpass is dominated by the Lyman-α line in the solar spectrum. The modeled response for Channel C is shown in Fig. 4.

All three science channels were also calibrated for response changes over their FOV.

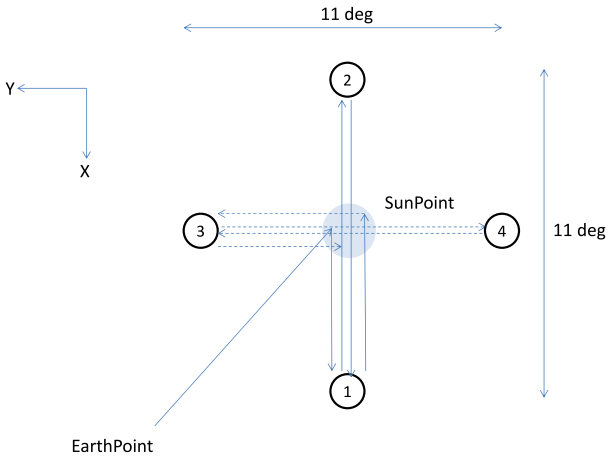

Fig. 5 Spacecraft pointing for the Cruciform Scan

4 Flight Operations and In-Flight Calibrations

Operations of the EUV monitor are simple. When the instrument is turned on, it produces telemetry data. The usefulness of that data can be broken down into three cases: (1) Sun within science FOV and aperture mechanism "open", (2) Sun within science FOV and aperture mechanism "closed", (3) Sun outside of glint-free FOV. For most of the MAVEN mission, case (1) will be the norm. Case (1) produces valid solar irradiance measurements. Case (2) is considered the "visible light calibration" and is planned to be performed once per week to track any changes in the visible light contribution to the total signal for each channel. Case (3) is considered "dark calibrations" where the non-illuminated signals (the combination of offsets and background signals) for each channel are compared against the permanently dark Channel D. No special maneuvers are planned to ensure Case (3) as it will occur frequently throughout the mission when the spacecraft points off the Sun for transmission of data to Earth or to engage in various non-Sun-pointed periapsis maneuvers.

Other special calibrations planned for the MAVEN mission include a "Cruciform Scan" and a "FOV Raster Scan". The Cruciform Scan involves off-pointing the spacecraft (and hence the EUV) boresight and slowly scanning in two orthogonal spacecraft axes (X and Y) from dark through the Sun-pointing to dark again to determine if the boresight of the EUV instrument has changed relative to the spacecraft pointing and to look for degradation across the full FOV. Figure 5 shows the Cruciform Scan. The slew rate is slow enough that the Sun does not move in the instrument FOV faster than 0.5 arc-min per each 1-sec integration. The Cruciform Scan is done during the Transition Phase after Mars Orbit Insertion, but before the start of the Science Phase, then repeated again once per year throughout the mission. If significant solar activity occurs during the scan, rendering it invalid for boresight determination the maneuver will have to be repeated.

The FOV Raster Scan involves a much finer mapping of the central portion of the FOV, making seven rows of 0.6° scans in the spacecraft Y axis spaced by 0.1° in the X axis. This allows for tracking of any changes in the response of the instrument over the nominal FOV. The FOV Raster Scan is illustrated in Fig. 6. As with the Cruciform Scan, the FOV Raster is done during Transition Phase and again annually through the mission.

The bandpasses on the MAVEN EUV monitor were chosen to match those of existing EUV instrumentation in Earth orbit. Channels A and C have identical filters and silicon detectors as channels on both the SORCE XPS and TIMED-SEE XPS. The bandpass of

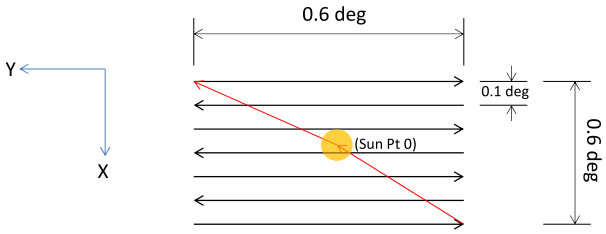

Fig. 6 Spacecraft pointing for the FOV Raster Scan

Channel C is also measured by SORCE SOLSTICE and the SDO-EVE MEGS-P channel. Channel A also has an overlapping bandpass with the SDO-EVE ESP. Channel B is similarly identical to the central order channel on the SDO-EVE ESP.

In-flight calibration of the EUV monitor measurements are accomplished through inter-comparisons with Earth-orbit-based instrumentation. Twice during the Cruise Phase of MAVEN to Mars the spacecraft is able to view the same face of the Sun as Earth-based assets, allowing for simultaneous measurements from both. At no other time during the primary mission will MAVEN and Earth be lined up with the Sun (although there are such alignments after the end of the primary mission if an extended mission is funded). Inter-comparisons of the simultaneous MAVEN EUV monitor measurements and the Earth-orbit measurements during the Cruise Phase allow for final adjustments of the responsivities of the MAVEN channels if there are any changes between ground calibration and flight.

While at Mars orbit, similar inter-comparisons can be made with Earth-based measurements by doing longer term averages (days to months) and shifting the measurements in time and distance. This will allow for tracking of any gross degradation of the MAVEN instrumentation until simultaneous aligned observations from Earth and Mars can be made again.

5 Data Products and Data Processing Algorithms

There are two public data products for the EUV monitor. These products are archived at the NASA Planetary Data System (PDS) in Common Data Format (CDF) files, along with documentation about the product generation and structure of the files. The Level 2 data product is the calibrated solar irradiance (Watts/m^2) in the broad bands of the three science channels at 1-second cadence. The PDS archive for the Level 2 product consists of daily CDF files. The Level 3 data product is a modeled full spectral irradiance (Watts/m^2/nm) in 1-nm bins from 0–190 nm both as a daily average and a 1-minute cadence. The Level 3 products are also one file per day each for the daily average spectrum and for the minutely data. Both Level 2 and Level 3 data products are presented as irradiances at the location of Mars at the times indicated in the products. The irradiances are *not* scaled to a fixed distance from the Sun.

The Level 2 band data product is the result of applying the responsivity calibrations to each of the science channels. The irradiance, E_i, in channel i is given by:

$$E_i = \frac{(I_{tot,i} - I_{vis,i} - I_{bkg,i})}{f_{FOV,i} \cdot \langle R_i \rangle} \cdot f_{Degrad,i}$$

where $I_{tot,i}$ is the total current measured in the channel (Amps); $I_{vis,i}$ is the fraction of the current due to out-of band or visible light determined through windowed aperture calibrations; $I_{bkg,i}$ is the background current due to temperature and particle radiation as calibrated

against the dark channel; $f_{FOV,i}$ is the relative response of the channel to off-pointing from the calibration FOV maps made at SURF, $f_{Degrad,i}$ is a correction factor included for possible time-dependent changes in the responsivity of the channel due to degradation, and $\langle R_i \rangle$ is the reported bandpass weighted response of the channel given by:

$$\langle R_i \rangle = \frac{\int_0^\infty R_i(\lambda) \cdot E(\lambda) \cdot d\lambda}{\int_{\lambda_1}^{\lambda_2} E(\lambda) \cdot d\lambda},$$

where R_i is the wavelength response of the channel as calibrated at SURF (and shown in Figs. 3 and 4) in Amps/(Watts/m^2), $E(\lambda)$ is the assumed shape of the solar spectrum (a reference spectrum), and the range λ_1 to λ_2 is the wavelength range or bandpass in which the irradiance is being reported. Note that the response of a channel depends on the solar spectral shape assumed. For the initial release of the data products a fixed reference spectrum for moderate solar activity is used based on a combination of TIMED-SEE and SDO-EVE measurements and modeling. It is planned that later versions of the data product will use multiple reference spectra for differing levels of solar activity. (Activity level reference spectra are currently being developed for the SDO-EVE program, but are not published yet.) The choice of reference spectra are particularly important for removing the short wavelength response of Channel A during flaring periods. Until the multiple reference spectra are used, the quality of the Channel A data during flares will be suspect due to this effect. During non-flaring times, however, the Channel A irradiances will only be minimally affected.

The Level 3 data product is a modeled spectral irradiance generated using a modified version of the Flare Irradiance Spectral Model (FISM) called FISM-Planetary (FISM-P). The original FISM (Chamberlin et al. 2007 and 2008) was an empirically derived proxy model based on observations made by the TIMED-SEE and SOLSTICE instruments. It used the best available proxies measured at Earth (or from Earth orbit) for each layer of the solar atmosphere contributing to the EUV spectral irradiance (namely the chromosphere, transition region, cool corona, and hot corona) to generate irradiances scaled to 1-AU for Earth from 0–190 nm at daily and 1-minute time cadences. The new FISM-P has the same wavelength and time resolution, but FISM-P will estimate irradiances throughout the solar system using weighted interpolation in time and location of the best available proxies, be they from Earth or from the MAVEN EUV monitor at Mars, or from any future instruments at other locations in the solar system.

Like the original FISM, FISM-P decomposes the irradiance into contributions from a minimum reference spectrum plus solar cycle variability plus solar rotational variability plus solar flare variability. Because the MAVEN EUV monitor is not measuring all the necessary proxies needed to drive the model at Mars, the longer-term (solar cycle and solar rotation) variability is mostly driven by proxies measured at Earth that are interpolated around to the heliospheric longitude of Mars at the time of the MAVEN measurements (primarily the MgII core-to-wing ratio and the F10.7 index). This interpolation requires Earth-based proxies from a solar rotation centered around the location of Mars at the time to which they are being interpolated. The Lyman-α irradiance measured at Mars by Channel C of the EUV monitor is also available for helping to determine daily irradiances. For the short term variability caused by flares, the coronal and hot coronal irradiances measured by Channels A and B, respectively, are used. In particular, Channel B responds very similarly to flares as the GOES Long (0.1–0.8 nm) channel which drives the Earth FISM flare variability.

6 Summary

The MAVEN EUV monitor measures the variability of the solar irradiance at Mars in three broad bandpasses that represent transition region, coronal, and hot coronal (or flaring) emissions from the Sun. These measurements are directly indicative of the variable EUV and soft X-ray input to the Mars atmosphere that drives variability in heating, ionization, and photodissociation that all contribute to atmospheric escape. In combination with interpolated Earth-based proxies, the EUV monitor measurements are used in the empirical FISM-P model to generate full spectral irradiances from 0–190 nm in 1-nm bins at 1-minute and daily time cadences, suitable for use in atmospheric models.

Acknowledgements The authors are grateful to the large number of people who have contributed to the success of this project. In particular we want to acknowledge all the engineers working on the EUV instrument and the Particles and Fields Package. The work was made under NASA MAVEN contract (NNH10CC04C).

References

L. Andersson, R.E. Ergun, G.T. Delory, A. Eriksson, J. Westfall, H. Reed, J. McCauly, D. Summers, D. Meyers, The Langmuir Probe and Waves (LPW) instrument for MAVEN. Space Sci. Rev. (2014, this issue). doi:10.1007/s11214-015-0194-3

S.M. Bailey, T.N. Woods, C.A. Barth, S.C. Solomon, L.R. Canfield, R. Korde, Measurements of the solar soft X-ray irradiance by the Student Nitric Oxide Explorer: first analysis and underflight calibrations. J. Geophys. Res. **105**(A12) (2000). doi:10.1029/2000JA000188

P.C. Chamberlin, T.N. Woods, F.G. Eparvier, Flare irradiance spectral model (FISM): daily component algorithms and results. Space Weather **5**(6) (2007). doi:10.1029/2007SW000316

P.C. Chamberlin, T.N. Woods, F.G. Eparvier, Flare irradiance spectral model (FISM): flare component algorithms and results. Space Weather **6**(5) (2008). doi:10.1029/2007SW000372

E.M. Gullikson, R. Korde, L.R. Canfield, R.E. Vest, Stable silicon photodiodes for absolute intensity measurements in the VUV and soft X-ray regions. J. Electron Spectrosc. Relat. Phenom. **80** (1996). doi:10.1016/0368-2048(96)02983-0

B.L. Henke, E.M. Gullikson, J.C. Davis, X-Ray interactions: photoabsorption, scattering, transmission, and reflection at $E = 50$–$30{,}000$ eV, $Z = 1$–92. At. Data Nucl. Data Tables **54** (1993). doi:10.1006/adnd.1993.1013

R. Korde, J. Geist, Quantum efficiency stability of silicon photodiodes. Appl. Opt. **26** (1987). doi:10.1364/AO.26.005284

R. Korde, L.R. Canfield, B. Wallis, Stable high quantum efficiency silicon photodiodes for vacuum-UV applications. Proc. SPIE Int. Soc. Opt. Eng. **932** (1988). doi:10.1117/12.946887

J.L. Lean, T.N. Woods, F.G. Eparvier, R.R. Meier, D.J. Strickland, J.T. Correira, J.S. Evans, Solar extreme ultraviolet irradiance: present, past, and future. J. Geophys. Res. **116**(A1) (2011). doi:10.1029/2010JA015901

T.N. Woods, G.J. Rottman, Solar ultraviolet variability over time periods of aeronomic interest, in *Atmospheres in the Solar System: Comparative Aeronomy*, ed. by M. Mendillo, A. Nagy, J.H. Waite (American Geophysical Union, Washington, 2002). doi:10.1029/130GM14

T.N. Woods, W.K. Tobiska, G.J. Rottman, J.R. Worden, Improved solar Lyman α irradiance modeling from 1947 through 1999 based on UARS observations. J. Geophys. Res. **105**(A12) (2000). doi:10.1029/2000JA000051

T.N. Woods, F.G. Eparvier, S.M. Bailey, P.C. Chamberlin, J. Lean, G.J. Rottman, S.C. Solomon, W.K. Tobiska, D.L. Woodraska, Solar EUV Experiment (SEE): mission overview and first results J. Geophys. Res. **110** (2005a). doi:10.1029/2004JA010765

T.N. Woods, G. Rottman, R. Vest, XUV Photometer System (XPS): overview and calibrations, in *The Solar Radiation and Climate Experiment (SORCE)*, ed. by T. Woods, V. George (Springer, Berlin, 2005b). doi:10.1007/0-387-37625-9_16

T.N. Woods, F.G. Eparvier, R. Hock, A.R. Jones, D. Woodraska, D. Judge, L. Didkovsky, J. Lean, J. Mariska, H. Warren, D. McMullin, P. Chamberlin, G. Berthiaume, S. Bailey, T. Fuller-Rowell, J. Sojka, W.K. Tobiska, R. Viereck, Extreme Ultraviolet Variability Experiment (EVE) on the Solar Dynamics Observatory (SDO): overview of science objectives, instrument design, data products, and model developments. Sol. Phys. **250** (2012). doi:10.1007/s11207-009-9487-6